

Domain structure dynamics of amorphous $\text{Fe}_{64}\text{Co}_{21}\text{B}_{15}$ and $\text{Co}_{77}\text{B}_{23}$ ribbons studied by three-dimensional neutron depolarization

J. P. Sinnecker^{a)}

Instituto de Física "Gleb Wataghin," UNICAMP, 13083-970—Campinas, SP, Brasil

R. Sato Turtelli^{b)} and R. Grössinger

Institut für Experimentalphysik, TU Wien, Wiedner Hauptstrasse 8-10, A-1040, Vienna, Austria

G. Badurek, P. Riedler, and S. Menhart

Institut für Kernphysik, TU Wien, Stadionallee 2, A-1020, Vienna, Austria

(Received 8 June 1998; accepted for publication 6 October 1998)

Relaxation phenomena related to domain structure dynamics in amorphous ferromagnetic $\text{Fe}_{64}\text{Co}_{21}\text{B}_{15}$, and $\text{Co}_{77}\text{B}_{23}$ samples were studied by time-resolved three-dimensional neutron depolarization and a conventional magnetic induction technique. Different initial domain structures were induced either by applying external stresses or by stress annealing. A theoretical model was developed to describe the observed time dependence of neutron depolarization upon passage through such samples. It is shown that the domain structure approaches the equilibrium state with stable domain wall positions at a rate that depends essentially both on the sample composition and on the induced magnetic anisotropy. © 1999 American Institute of Physics.

[S0021-8979(99)01402-4]

I. INTRODUCTION

The reversible relaxation of the initial magnetic permeability after nucleation of a new magnetic domain structure in a previously saturated sample (also known as "permeability aftereffect" or "disaccommodation") is a characteristic feature of soft ferromagnetic amorphous alloys, which can be observed over a wide temperature range. Disaccommodation has been studied both theoretically and experimentally for relaxation times as short as 10^{-5} s as well as for much larger times by means of the conventional impulsive technique.¹⁻⁶ For times longer than 10^{-3} s after removal of the external magnetic field, the reversible decay of the permeability with a quasilogarithmic behavior could be interpreted as being of diffusive type, originating from thermally activated processes of directional ordering of atoms or atomic groups with broadly distributed activation energies.^{3,4} For times shorter than 10^{-3} s ($10^{-5} < t < 10^{-3}$ s), in a sample exposed to a 200 MPa external stress, Allia *et al.* observed a fast magnetic relaxation effect, represented by a quasiexponential decay.^{2,5,6} This fast decay could not be attributed to processes with a single, well-defined activation energy because the measured decay time constant was essentially independent of temperature. This rapid relaxation was explained by a change of the number of actively moving domain walls. However, there is still a lack of convincing experiments to account for such a domain pattern change during this reduced time scale.

Neutron depolarization (ND) is a powerful technique to investigate both static and dynamic magnetic structures of bulk materials in the micron and submicron region.⁷⁻⁹ Using this technique Sinnecker *et al.*^{10,11} could observe relaxation

effects in a series of amorphous alloys without requiring an ac magnetic field to be applied during the relaxation process. In this work we present results obtained by time-resolved three-dimensional (3D)-neutron depolarization in amorphous ferromagnetic ribbons of $\text{Fe}_{64}\text{Co}_{21}\text{B}_{15}$ and $\text{Co}_{77}\text{B}_{23}$. In order to detect magnetic flux variations, which are associated with domain structure changes simple voltage induction measurements were performed simultaneously in the same samples. A simple theoretical model was developed to interpret the experimental results. It will be shown that the observed relaxation effects are related to the nucleation and dissipative planar motion of domain walls.

II. NEUTRON DEPOLARIZATION

Neutron depolarization (ND) is a powerful technique to study the magnetic domain structure within the bulk of magnetic materials and not only at their surface. In a ND experiment one records the change of the polarization vector of a polarized neutron beam upon transmission through a magnetically ordered sample. ND in ferromagnetic media can be described equally well either by a scattering approach¹² or by a semiclassical spin rotation formalism.¹³ We restrict our consideration in what follows to the latter. It is based essentially on the Larmor precession of the polarization vector \mathbf{P} upon neutron passage through a region of uniform magnetic field \mathbf{B} according to the equation of motion

$$\frac{d\mathbf{P}}{dt} = \gamma\mathbf{P} \times \mathbf{B}, \quad (1)$$

where $\gamma = -1.833 \times 10^8$ rad/s T is the gyromagnetic ratio of the neutron. Since the magnitude and direction of the local magnetization within each domain of a ferromagnetic sample can be assumed to be constant, the change of the initial neu-

^{a)}Permanent address: Instituto de Física, Universidade Federal do Rio de Janeiro, Caixa Postal 68528, CEP:21945-970 Rio de Janeiro, Brasil.

^{b)}Electronic mail: sato@pop.xphys.tuwien.ac.at

tron polarization vector $\mathbf{P}(0)$ passing through a single domain of thickness d_k can be described by the relation

$$\mathbf{P}(t_k) = \mathbf{D}_k(\mathbf{n}_k, \omega t_k) \mathbf{P}(0), \quad (2)$$

where $t_k = d_k/v$ is the transmission time of a neutron with velocity v through that particular domain, \mathbf{n} is a unit vector

in the direction of the domain magnetization and $\omega = \gamma|B_s|$ is the Larmor precession frequency, which is assumed to be the same in all domains due to their identical saturation induction B_s . The matrix \mathbf{D}_k is a pure rotation matrix ($|\det \mathbf{D}_k| = 1$) which can be expressed in terms of the magnetization direction cosines as

$\mathbf{D}_k(\mathbf{n}_k, \omega t_k)$

$$= \begin{bmatrix} 1 - (1 - \cos \omega t_k)(1 - n_{kx}^2) & (1 - \cos \omega t_k)n_{kx}n_{ky} - n_{kz} - n_{kz} \sin \omega t_k & (1 - \cos \omega t_k)n_{kx}n_{kz} + n_{kx} \sin \omega t_k \\ (1 - \cos \omega t_k)n_{kx}n_{ky} + n_{kz} \sin \omega t_k & 1 - (1 - \cos \omega t_k)(1 - n_{ky}^2) & (1 - \cos \omega t_k)n_{ky}n_{kz} - n_{kx} \sin \omega t_k \\ (1 - \cos \omega t_k)n_{kx}n_{kz} - n_{ky} \sin \omega t_k & (1 - \cos \omega t_k)n_{ky}n_{kz} + n_{kx} \sin \omega t_k & 1 - (1 - \cos \omega t_k)(1 - n_{kz}^2) \end{bmatrix}. \quad (3)$$

Since for thermal neutrons the domain wall thickness (δ) in all ferromagnetic materials is negligible compared to the distance necessary for one full Larmor rotation, the transition of the neutron polarization vector from one domain to the next occurs almost completely nonadiabatically, i.e., without any significant change of its orientation. Consequently, the net effect of N domains sequentially traversed by an infinitely thin neutron beam can be described as a product of N rotation matrices of the type of Eq. (3), which is still of purely rotational character.

However, averaging over many trajectories distributed at random across the beam area yields the so-called depolarization matrix

$$\mathbf{D} = \left\langle \prod_{n=1}^N \mathbf{D}_n \right\rangle \quad (4)$$

which in general is not a pure rotation matrix ($|\det \mathbf{D}| \leq 1$).⁸ There $N = L/\langle d_i \rangle$ is the mean number of domains traversed by the individual neutron trajectories and the brackets denote the average over the neutron beam cross section. The degree of depolarization of the beam then depends crucially on the complexity of the domain structure and the thickness of the sample. While spin precessions around the locally fluctuating magnetic induction lead to an effective depolarization, i.e., to a reduction of the length of the polarization vector ($|\mathbf{P}| \leq 1$), the mean magnetization of the sample merely causes a rotation of \mathbf{P} .

Assuming statistical independence between neighboring domains, Rekveldt¹⁴ could formulate a theoretical depolarization matrix of a multidomain ferromagnetic specimen in terms of the mean square direction cosines $\langle n_x^2 \rangle$, $\langle n_y^2 \rangle$, $\langle n_z^2 \rangle$ of the domain magnetization, the mean reduced induction $m = \langle B_k \rangle / B_s$ of the sample, and the quantity $B_s^2 \langle d_k \rangle$. The reverse procedure, namely to derive these essential domain structure parameters from the experimentally measured depolarization matrix, is possible only if the average domain size $\langle d_k \rangle$ is small enough to fulfill the condition $\omega \langle d_k \rangle / v = \pi$. For correlated domain structures the situation is much more complicated, however, and no generally applicable, recipe-like procedure exists to invert the experimental data. Another major complication in interpreting ND measure-

ments arises from the fact that even for completely isotropic domain structures the depolarization effect is intrinsically anisotropic.¹² In that respect the recently proposed tensorial neutron magnetic tomography¹⁵ probably might become an important extension of the ‘‘classical’’ depolarization method.

Evidently, to measure all nine elements D_{ij} ($i, j = x, y, z$) of the 3×3 depolarization matrix \mathbf{D} an experimental setup is required where the polarization of the incident neutron beam can be oriented successively in any of the three directions of space and where also all three components of the final polarization vector after transmission through the sample can be analyzed separately. Here the indices i and j refer to the respective polarization orientation before and the analyzed polarization component behind the sample. The concept of ‘‘dynamical’’ neutron depolarization is to record the elements of \mathbf{D} via a multichannel counter data acquisition system as a function of time after some periodic excitation of the sample. This allows to study relaxation phenomena of the domain structure at real-time scales ranging typically from some microseconds to several hours.

III. EXPERIMENTAL

3D dynamical neutron depolarization experiments were performed using the crystal polarimeter setup at the 250 kW TRIGA reactor of the Atomic Institute of the University of Technology Vienna, which is shown schematically in Fig. 1. The incident beam with a mean wavelength $\lambda = 0.16$ nm and a relative monochromaticity $\Delta\lambda/\lambda \approx 1.5\%$ propagates along the $+\hat{y}$ direction. It is polarized in $+\hat{z}$ direction by Bragg reflection at a magnetized Heusler-alloy (Cu_2MnAl) crystal and confined to a diameter of 1 cm by a Cd diaphragm. The sample ribbon is mounted inside of a specially designed sample holder that allows the application of both a pulsed homogeneous magnetic field and a static mechanical stress along the ribbon axis (\hat{z} direction). The ribbon plane was oriented perpendicular to the beam, i.e., coinciding with the $\hat{x}\hat{z}$ plane. An additional compensated pick-up coil system wound around the sample region serves to detect any signals that are induced by the sample’s magnetic response on the discontinuously applied field. The central part of the sample

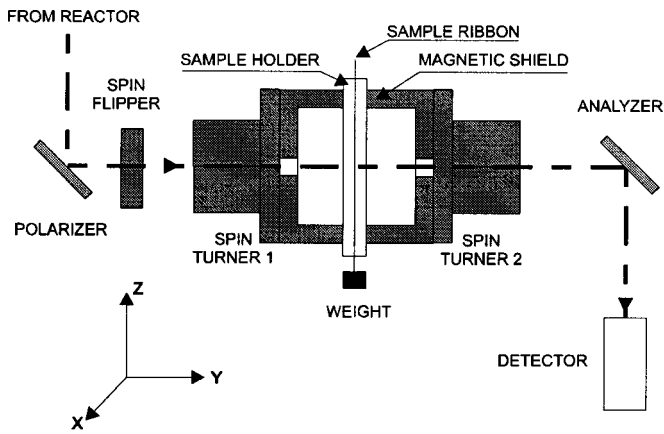


FIG. 1. Schematic drawing of the depolarization setup at the 250 kW research reactor in Vienna.

holder is placed within a soft-magnetic iron cube (with properly arranged holes at the beam entrance and exit and also for the extended parts of the sample holder) in order to suppress the disturbing influence of any external magnetic stray fields. Just in front and behind this shielding cube, spin-turn devices are attached to allow for an orientation of the incident neutron polarization vector successively into the \hat{x} , \hat{y} , and \hat{z} direction, and also to project any of the three spatial components of the final polarization vector behind the sample onto the direction of the analyzer. In this way, we could measure successively all nine elements of the depolarization matrix \mathbf{D} . Using a direct current (dc)-coil spin flipper¹⁶ with an efficiency $e \cong 99\%$ the incident beam polarization could be inverted and from the neutron intensities I^+ and I^- measured with flipper “OFF” and “ON,” respectively, the depolarization matrix elements can be calculated according to

$$D_{ij} = \frac{I_{ij}^+ - I_{ij}^-}{e(I_{ij}^+ + I_{ij}^-)} \quad (i, j = x, y \text{ or } z), \quad (5)$$

where the indices i and j , as mentioned already, refer to the respective orientation of the polarization vector before and its analyzed component after transmission through the sample. Under the plausible assumption that the small but unavoidable deviations of the “empty depolarization” matrix \mathbf{D}_e , which is measured without sample, from the unit matrix are symmetric with respect to the pre- and postsample beam trajectories, the effective depolarization matrix of the sample is found by the correction $\mathbf{D}_{\text{eff}} = \mathbf{D}_e^{-1/2} \mathbf{D} \mathbf{D}_e^{-1/2}$.

In order to detect magnetic relaxation effects a pulsed magnetic saturation field was periodically applied along the sample’s \hat{z} direction for duration of 500 μs , followed by a 2500- μs -long field-free interval. The rise and fall times of this field pulses were 17 and 10 μs , respectively. The pulse amplitude of 200 A/m was higher than the coercivity of all investigated amorphous ferromagnetic ribbons.¹⁷ At each rising edge of the pulse the multichannel counter was retriggered as to store the detected neutron intensity in 120 sequential time channels, each of 25 μs width. Thus within a total measuring time of 1 h 1.2×10^6 cycles were completed, corresponding to a total accumulation time of 30 s for each channel. Running this measuring scheme both for flipper ON

TABLE I. Sample characteristics.

Sample	Cross section (m^2)	Magnetostriction λ_s	Length (cm)
$\text{Fe}_{64}\text{Co}_{21}\text{B}_{15}$	2.8×10^{-7}	36.1×10^{-6}	50
$\text{Co}_{77}\text{B}_{23}$	2.1×10^{-7}	-3.6×10^{-6}	50

and OFF thus allowed to record successively the time evolution of all nine elements of the depolarization matrix.

All our samples were melt-spun amorphous ribbons, kindly supplied by the Slovakian Academy of Sciences in Bratislava, as part of the PECO joint program. The compositions and the characteristics of the samples are given in Table I. Depolarization measurements as a function of time were carried for $\text{Fe}_{64}\text{Co}_{21}\text{B}_{15}$ and $\text{Co}_{77}\text{B}_{23}$ samples, as well as for the empty sample holder, i.e., without sample but with applied pulsed magnetic field. The measurements were performed with and without external stress ($\sigma = 0, 87, \text{ and } 199$ MPa), which was applied along the samples’ longitudinal axis by a weight clamped to its lower lying end.

One $\text{Fe}_{64}\text{Co}_{21}\text{B}_{15}$ sample, which had been thermally annealed at 300 $^\circ\text{C}$ for 4 h with an applied stress of 500 MPa in order to induced a large anisotropy, was measured without external stress. Scanning electron microscopy (SEM) images of this sample, revealed a particularly regular domain structure consisting of large antiparallel domains oriented along the longitudinal axis of the ribbon.¹⁸ The other samples ($\text{Fe}_{64}\text{Co}_{21}\text{B}_{15}$ and $\text{Co}_{77}\text{B}_{23}$) were used in the as-cast state, exhibiting a complex finger print domain structure.⁸ Simultaneous depolarization and magnetic induction measurements were performed with the $\text{Fe}_{64}\text{Co}_{21}\text{B}_{15}$, and $\text{Co}_{77}\text{B}_{23}$ as-cast samples. There the induced voltage in a compensated pick-up coil system wound around the sample was recorded with a digital storage oscilloscope.

IV. RESULTS AND DISCUSSIONS

Figure 2(a) shows the time dependence of all nine matrix elements in the absence of a sample. As long as there is no magnetic field applied the measured depolarization matrix is proportional to the unit matrix. The deviation of the diagonal elements from the ideal value 1 is simply due to the fact that the incident beam is not completely polarized. As expected theoretically according to Eq. (3), a magnetic field pulse along the \hat{z} axis has a strong but opposite effect on the two off-diagonal matrix elements D_{xy} and D_{yx} and (a smaller) one of equal sign on the two diagonal elements D_{xx} and D_{yy} . All other matrix elements are not affected by the field and hence are constant in time. A homogeneous magnetic field cannot cause a depolarization of the beam but only a rotation of the polarization vector. Since the determinant of a pure rotation matrix is always identical to 1, the determinant of this measured “empty matrix” should not change even during the application of the field. Figure 2(b) clearly demonstrates this expected behavior, implicitly indicating the correct function of the experimental setup.

The time dependence of the depolarization matrix of a $\text{Fe}_{64}\text{Co}_{21}\text{B}_{15}$ sample measured at an applied mechanical stress of $\sigma = 87$ MPa is shown in Fig. 3, where the correction

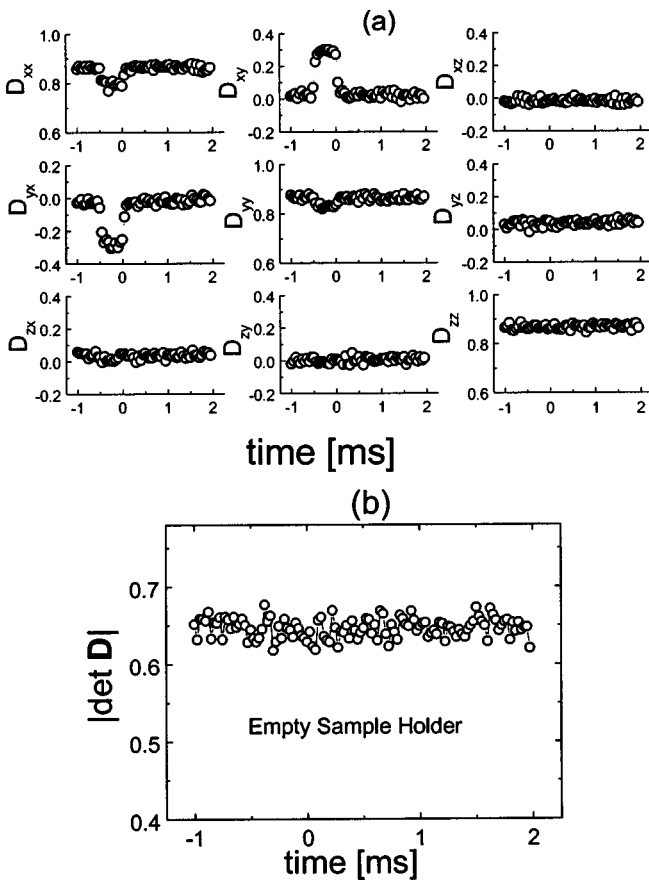


FIG. 2. (a) Dynamic measurements of the empty depolarization matrix. Pulse time $t = 500 \mu\text{s}$; (b) time evolution of the determinant of the empty depolarization matrix.

for the empty matrix has been already carried out. As can be seen, element D_{zz} obviously is not affected by the longitudinally applied field and its value is very close to 1. This result is compatible with the assumption that the applied stress induces a highly oriented structure of domains that are aligned either parallel or antiparallel to the stress axis. In Fig. 4 the time evolution of the determinants is plotted which have been calculated from the dynamically measured depolariza-

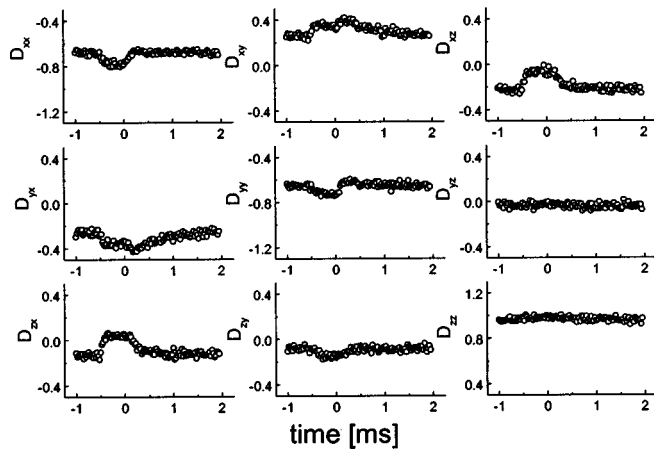


FIG. 3. Dynamic depolarization matrix of a $\text{Fe}_{64}\text{Co}_{21}\text{B}_{15}$ as-cast sample with $\sigma = 87 \text{ MPa}$.

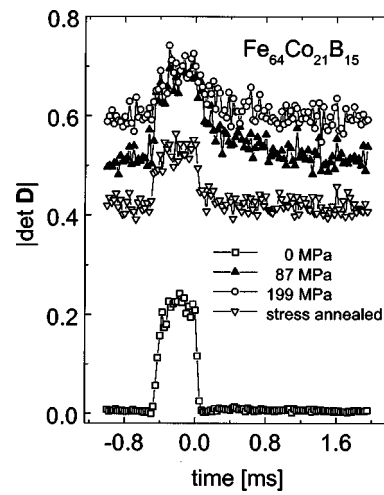


FIG. 4. Time evolution of the determinant of the depolarization matrix measured for $\text{Fe}_{64}\text{Co}_{21}\text{B}_{15}$ samples at $\sigma = 0, 87, 199 \text{ MPa}$ and for a stress annealed sample.

tion matrices of $\text{Fe}_{64}\text{Co}_{21}\text{B}_{15}$ for $\sigma = 0, 87,$ and 199 MPa . For the unstressed state ($\sigma = 0 \text{ MPa}$) one can see that outside the time interval where the field is applied (“field region”) the determinant is zero valued, meaning that the transmitted beam is fully depolarized. This complete loss of beam polarization in the absence of any external magnetic field or mechanical stress is caused by an irregular domain structure with lots of closure domains, which is essentially governed by local fluctuations of the long range internal stresses.¹⁹ The latter inevitably arise during the production process of such amorphous samples. The observable increase of the determinant during the application of the field results from the increase of the net magnetization of the sample as well as from the induction of a more regular domain structure.^{8,19}

For $\sigma = 87 \text{ MPa}$ one can see immediately the effect of the external tension on the domain structure. Compared to the stress-free measurement, the region without field exhibits a significant increase of the determinant due to the stress-induced regularity of the domain structure. Because of the positive magnetostriction constant of this sample collinear domain alignment with respect to any applied stress occurs. During the application of field the regularity is further enhanced due to the associated magnetization process, and hence the value of the determinant increases even more. However, after removal of the field this excess regularity, i.e., the magnetic remanence of the sample, is not stable and the determinant relaxes back to its stress-induced equilibrium value. Such a relaxation process is also observed in the measurement at $\sigma = 199 \text{ MPa}$, where in the field-free region, as one obviously expects, the equilibrium determinant exceeds the values obtained at $\sigma = 0$ and 87 MPa . The preannealed sample, on the other hand, when measured without applied stress, yields a depolarization in the field-free region which is of the same order of magnitude than that of the stressed samples, indicating the presence of a similar domain structure.

Analogous measurements were performed with a $\text{Co}_{77}\text{B}_{23}$ sample, whose magnetostriction is negative. The time dependence of the depolarization matrix determinant of

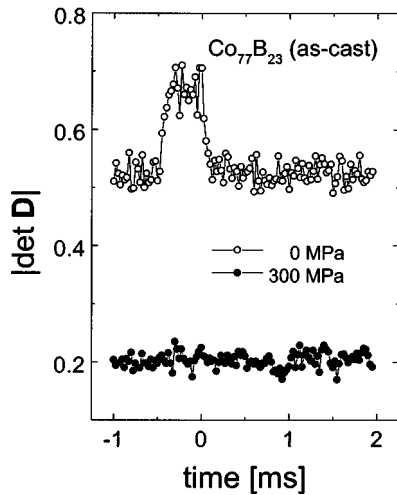


FIG. 5. Time evolution of the depolarization matrix measured in a $\text{Co}_{77}\text{B}_{23}$ as cast sample at $\sigma=0$ and 300 MPa.

this sample is plotted in Fig. 5 for $\sigma=0$ and 300 MPa. The observed reduction of the determinant with increasing external stress is fully compatible with the fact that because of the negative magnetostriction the domains do not align along but instead at right angle to the stress axis. Although the 200 A/m longitudinal field pulse is perpendicular to these domains it is obviously not sufficient to enforce their rotation to the \hat{z} direction.

Phenomenologically the relaxation effect observed in the dynamic 3D neutron depolarization measurements is originated from a change in the magnetization distribution in the interior of the samples, and it reflects the stabilization of the domain structures. During the application of the magnetic field the sample is nearly saturated. Immediately after the sudden removal of the field the remaining remanent magnetization starts to decrease gradually with increasing time. This relaxation of the magnetization can be connected with some basic processes as:

- (1) *Nucleation* of domain walls,
- (2) *Displacement* of already existing domain walls,
- (3) *Rotation* of the local magnetization inside of already existing domains.

Generally speaking, in amorphous materials with positive magnetostriction the nucleation of domain walls should take place very fast within times of the order of 10^{-6} – 10^{-4} s. Taking into account that in our dynamic ND experiments the time resolution was adequate to study relaxation phenomena at a time scale of about 100 μs , only processes (2) and (3) need to be considered here.

The theoretical depolarization matrix and its time evolution were calculated for each of these two processes and then compared with the results of our measurements. The theoretical depolarization matrix can be derived by considering a hypothetical domain structure and by calculating the change of the polarization vector upon passage through such a structure by means of Eqs. (1) and (2). To determine the time

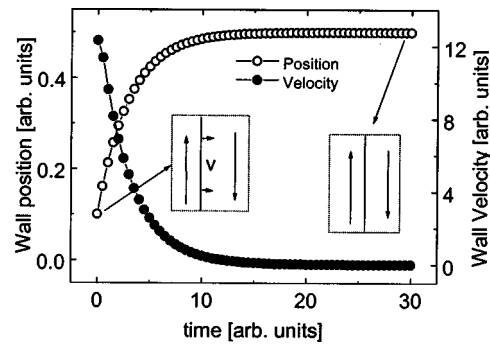


FIG. 6. Model of a simple domain wall configuration: (a) domain position; (b) domain wall velocity.

evolution of the magnetization a relaxation model was assumed and then the theoretical depolarization matrix for each time interval was calculated step by step.

V. DOMAIN WALL DISPLACEMENT MODEL

Let us assume a long ribbon-shaped sample with a thickness of about 20 μm (like that of our actual samples) in the same geometrical arrangement that was chosen in our experimental setup. Let us furthermore assume a simple domain structure that is composed of only two domains, separated by a single domain wall. This domain wall should be considered to be a 180° wall, which is fairly reasonable for a stressed positive magnetostrictive sample. The equilibrium position of this longitudinal wall shall be at the center of the sample. Application of a longitudinal magnetic field forces this domain wall to move into a specific direction (e.g., the \hat{x} axis). Subsequent sudden removal of this field is followed by a relaxation process since the wall will return to its equilibrium position with some velocity $v(t)$. It is plausible to assume that the rate of approaching equilibrium decreases linearly with decreasing distance from the equilibrium position, which corresponds to an exponentially decreasing wall velocity. Figure 6 shows the velocity and the position of such a domain wall as a function of time according to our model. For simplicity we have chosen arbitrary relative units. The width of our hypothetical ‘‘sample’’ was defined as 1 unit, the origin of coordinates was set at $x=0$. This means that the equilibrium position of the domain wall is at $x=0.5$. Given these conditions the influence of these two domain portions on the transmitted neutron spin can be calculated theoretically. In one of them the magnetization points towards the $+\hat{z}$ direction, while in the other one it points to the $-\hat{z}$ direction. The direction cosines are thus $\mathbf{n}_1=(0,0,1)$ for the first domain, and $\mathbf{n}_2=(0,0,-1)$ for the other. Taking into account the known saturation induction $B_S=1.2$ T one obtains immediately from Eq. (3) the two pure rotation matrices

$$\mathbf{D}_{+z} = \begin{bmatrix} -0.0954 & -0.995 & 0 \\ 0.995 & -0.0954 & 0 \\ 0 & 0 & 1 \end{bmatrix}$$

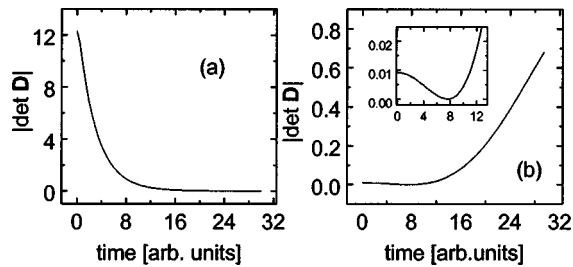


FIG. 7. Calculated time evolution of the determinant of the theoretical depolarization matrix of the domain wall displacement model (a), and of the rotation model (b).

$$\mathbf{D}_{-z} = \begin{bmatrix} -0.0954 & 0.995 & 0 \\ -0.995 & -0.0954 & 0 \\ 0 & 0 & 1 \end{bmatrix}, \quad (6)$$

which have both a determinant equal to 1.

To derive the effective depolarization matrix according to Eq. (4) an averaging over the beam cross section has to be performed. In our simplified single layer domain model this means just to take into account the relative portions of the two regions with upward and downward magnetization. Since per definition the time-dependent position $x(t)$ of the domain wall can take a value between 0 and 1, the time dependence of the depolarization matrix can be expressed by

$$\mathbf{D}(t) = x(t)\mathbf{D}_{+z} + [1 - x(t)]\mathbf{D}_{-z}. \quad (7)$$

Figure 7(a) shows the time evolution of the determinant of this theoretically derived depolarization matrix of our hypothetical sample, assuming $x=0$ as start position and $x=0.5$ as equilibrium position. Its behavior is obviously very similar to the experimental results, therefore this model of domain wall displacement in spite of its extreme simplicity is a reasonably good candidate for a correct theoretical description of the observed relaxation process.

VI. MODEL OF LOCAL MAGNETIZATION ROTATION

Let us now consider the model of local magnetization rotation. Like in the previous model a domain structure is assumed which is composed of two domains with mutually opposite magnetization directions, separated by a single 180° domain wall. Initially it is assumed that the domain wall is inclined at a certain angle relative to the longitudinal ribbon axis. Here the change of local magnetization with time shall be related to a rotation of the local magnetization, and hence of the domain wall too. When an external field is applied along the ribbon axis the domain magnetization directions begin to rotate until they are aligned either parallel or antiparallel to the field. By switching off the applied field, the local magnetization vector will have a tendency to rotate back to its equilibrium position within some characteristic time interval. In this case, the position of the wall remains constant but its direction changes with time. Using the same mathematical procedure as before, the time evolution of the depolarization matrix and its determinant were calculated for this specific model. The behavior of the time dependence of the determinant, which is plotted in Fig. 7(b), is completely opposite to what has actually been measured (see Fig. 4).

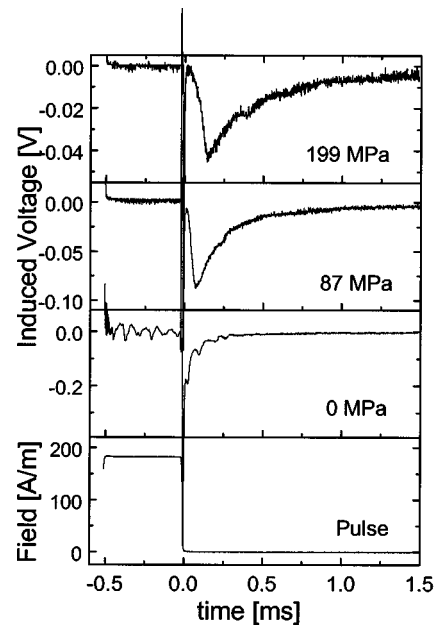


FIG. 8. Induced voltage in the compensated pick-up coil as function of time for the $\text{Fe}_{64}\text{Co}_{21}\text{B}_{15}$ as-cast ribbon at different values of the applied external stress. The lowest curve shows the time structure of the pulsed magnetic field.

This means that such a model is obviously completely inadequate to describe the observed temporal change of the magnetization of our soft-magnetic amorphous ribbons.

Figure 8 shows the voltage that is induced in the pick-up coil system as a function of time for the $\text{Fe}_{64}\text{Co}_{21}\text{B}_{15}$ as-cast sample at different applied external stress values. Additionally the time dependence of the applied magnetic field pulse is plotted in the same figure. Just after the end of the field pulse a clear voltage peak can be observed in this positive

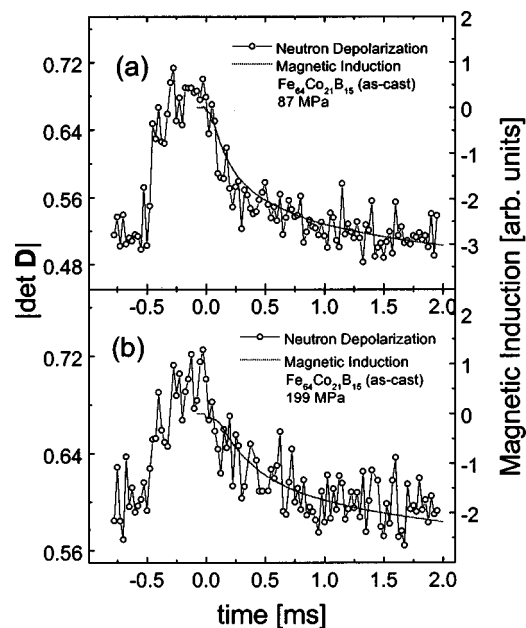


FIG. 9. Magnetic flux obtained from the integral of the induced voltage (full line) and determinant of the depolarization matrix (circles) for the $\text{Fe}_{64}\text{Co}_{21}\text{B}_{15}$ sample stressed at (a) $\sigma=87$ and (b) $\sigma=199$ MPa.

magnetostrictive sample, whereas no such induction peak occurs when the negative magnetostrictive $\text{Co}_{77}\text{B}_{23}$ ribbon is investigated. The induction peak appears after the end of the magnetic pulse where an external field no longer persists. Therefore the induction signal comes directly from the flux variation that is caused by the change of magnetic structure of the sample. Because the induced voltage is proportional to the time derivative of the magnetic flux, an integration with respect to time yields the magnetic flux as a function of time, which in turn is proportional to the mean magnetic induction within the sample. In Figs. 9(a) and 9(b) the relaxation behavior of the depolarization matrix determinant for the $\text{Fe}_{64}\text{Co}_{21}\text{B}_{15}$ as-cast sample stressed at $\sigma=87$ and 199 MPa, respectively, is plotted together with the decaying mean magnetic induction that has been obtained by integration of the voltage induced in the pick-up coils. There is an obviously perfect agreement between these two results, indicating that both are governed by the same (de)magnetization process. A quantitative analysis of the stress dependence of the depolarization and the magnetic relaxation rate as well as that of the peak height of the induction voltage will be subject of a forthcoming article.

VII. CONCLUSIONS

Short time relaxation effects in amorphous soft-magnetic ribbons with different initial domain structures were studied both by three-dimensional neutron depolarization and by a magnetic induction technique. A simple domain structure model was developed to describe the observed time evolution of neutron depolarization. The results show that the time dependence of the magnetization, due to the stabilization of the domain wall to an equilibrium position, depends on the sample composition and on the stress induced anisotropy.

ACKNOWLEDGMENTS

The authors thank Dr. Zaveta and Dr. Kraus from Prague for supplying the annealed sample and also for its SEM characterization. This work was supported by the Austrian Fonds zur Förderung der Wissenschaftlichen Forschung (Project No. P9707-PHY) and partly by Hochschuljubiläumsstiftung der Stadt Wien (Project No. H-00025/95). J. P. Sinnecker thanks FAPESP of Brasil for a fellowship grant.

- ¹R. Sato Turtelli and F. Vinai, *Rev. Bras. Fis.* **20**, 203 (1990).
- ²P. Allia, C. Beatrice, P. Mazzetti, and F. Vinai, *J. Magn. Magn. Mater.* **54–57**, 273 (1986).
- ³P. Allia and F. Vinai, *Phys. Rev. B* **33**, 422 (1986).
- ⁴H. Kronmüller, *Philos. Mag. B* **48**, 127 (1983).
- ⁵P. Allia, C. Beatrice, P. Mazzetti, and F. Vinai, *Appl. Phys. Lett.* **51**, 142 (1987).
- ⁶P. Allia and F. Vinai, *Philos. Mag. B* **61-4**, 763 (1990).
- ⁷G. M. Drabkin, E. I. Zabidarov, Ya. A. Kasman, and A. I. Okorokov, *J. Exp. Theor. Phys.* **29**, 261 (1969).
- ⁸A. Veider, G. Badurek, R. Grössinger, and H. Kronmüller, *J. Magn. Magn. Mater.* **60**, 182 (1986).
- ⁹M. de Jong, L. Köszegi, J. Sietsma, M. Th. Rekveldt, and A. van den Beukel, *J. Magn. Magn. Mater.* **152**, 326 (1996).
- ¹⁰J. P. Sinnecker, R. Sato Turtelli, R. Grössinger, P. Riedler, and G. Badurek, *Nanostructured and Non-Crystalline Materials*, edited by M. Vázquez and A. Hernando, 1995 (unpublished), Vol. 1, p. 562.
- ¹¹J. P. Sinnecker, G. Badurek, R. Grössinger, P. Riedler, and R. Sato Turtelli, *J. Magn. Magn. Mater.* **140–144**, 331 (1995).
- ¹²S. V. Maleev and V. A. Ruban, *Sov. Phys. JETP* **35**, 222 (1972).
- ¹³R. Rosman and M. Th. Rekveldt, *Z. Phys. B* **79**, 61 (1990).
- ¹⁴M. Th. Rekveldt, *Z. Phys.* **259**, 391 (1973).
- ¹⁵M. Hochhold, H. Leeb, and G. Badurek, *J. Phys. Soc. Jpn.* **65**, Suppl. A, 292 (1996).
- ¹⁶G. Badurek, *Nucl. Instrum. Methods* **189**, 543 (1981).
- ¹⁷Ch. Polak, J. P. Sinnecker, R. Grössinger, M. Knobel, and R. Sato Turtelli, *J. Appl. Phys.* **73**, 5272 (1993).
- ¹⁸1st-Year Progress Report of PECO-COPERNICUS Programme, Contract: CIPA-CT93-0239 (1995) 49.
- ¹⁹H. Kronmüller, *At. Energ. Rev. Suppl.* **1**, 255 (1981).